Glypican-5 stimulates rhabdomyosarcoma cell proliferation by activating Hedgehog signaling

Fuchuan Li,[1,2] Wen Shi,[1,2] Mariana Capurro,[1,2] and Jorge Filmus[1,2]

[1]Division of Molecular and Cell Biology, Sunnybrook Research Institute, and [2]Department of Medical Biophysics, University of Toronto, Toronto, Ontario M4N3M5, Canada

Glypican-5 (GPC5) is one of the six members of the glypican family. It has been previously reported that GPC5 stimulates the proliferation of rhabdomyosarcoma cells. In this study, we show that this stimulatory activity of GPC5 is a result of its ability to promote Hedgehog (Hh) signaling. We have previously shown that GPC3, another member of the glypican family, inhibits Hh signaling by competing with Patched 1 (Ptc1) for Hh binding. Furthermore, we showed that GPC3 binds to Hh through its core protein but not to Ptc1. In this paper, we demonstrate that GPC5 increases the binding of Sonic Hh to Ptc1. We also show that GPC5 binds to both Hh and Ptc1 through its glycosaminoglycan chains and that, unlike GPC3, GPC5 localizes to the primary cilia. Interestingly, we found that the heparan sulfate chains of GPC5 display a significantly higher degree of sulfation than those of GPC3. Based on these results, we propose that GPC5 stimulates Hh signaling by facilitating/stabilizing the interaction between Hh and Ptc1.

Introduction

Rhabdomyosarcoma (RMS) is the most common soft-tissue sarcoma in children and adolescents, accounting for ∼5–10% of all pediatric solid malignancies (Breitfeld and Meyer, 2005). RMSs resemble developing skeletal muscle, and they are broadly divided into two main subgroups based on their histology: alveolar and embryonal.

Recently, Williamson et al. (2007) showed that the gene encoding glypican-5 (GPC5), a member of the glypican family, was amplified in ∼20% of patients with alveolar RMS and that this glypican was overexpressed in all 85 RMS patients included in their study compared with normal muscle. Moreover, these authors showed that down-regulation of GPC5 expression by RNAi inhibits the proliferation rate of RMS cells.

Glypicans are a family of proteoglycans that are linked to the exocytoplasmic surface of the plasma membrane via a glycosylphosphatidylinositol anchor (Filmus and Selleck, 2001; Song and Filmus, 2002; Filmus et al., 2008). Six glypicans have been identified in mammals (GPC1 to GPC6) and two in *Drosophila melanogaster* (Dally and Dlp; Paine-Saunders et al., 1999; Veugelers et al., 1999; Filmus et al., 2008). Like all proteoglycans, glypicans display a variable number of glycosaminoglycan (GAG) chains. The core proteins of glypicans are characterized by a similar size (60–70 kD) and a highly conserved localization of 14 cysteine residues. In addition, all the insertion sites for the GAG chains are found within the last 60 amino acids, placing these chains close to the cell surface (Filmus et al., 2008). Generally, glypicans carry heparan sulfate (HS) chains, but GPC5 also displays chondroitin sulfate (CS) chains (Saunders et al., 1997).

Glypicans regulate the signaling activity of various morphogens/growth factors, including Wnts (Lin and Perrimon, 1999; Tsuda et al., 1999; Ohkawara et al., 2003; Song et al., 2005), Hedgehogs (Hh's; Desbordes and Sanson, 2003; Lum et al., 2003; Han et al., 2004; Beckett et al., 2008; Gallet et al., 2008; Yan et al., 2010), and bone morphogenic proteins (Jackson et al., 1997; Kreuger et al., 2004; Akiyama et al., 2008). Genetic and biochemical studies have shown that glypicans regulate morphogen/growth factor signaling at the level of ligand receptor interaction (Desbordes and Sanson, 2003; Song et al., 2005). The picture that is emerging from the recent literature is that the specific function of a particular glypican depends on the structural

Correspondence to Jorge Filmus: jorge.filmus@sri.utoronto.ca

Abbreviations used in this paper: 2AB, 2-aminobenzamide; CS, chondroitin sulfate; CSase, chondroitinase; GAG, glycosaminoglycan; Hh, Hedgehog; HS, heparan sulfate; HSase, heparitinase; Ptc1, Patched 1; RMS, rhabdomyosarcoma; Shh, Sonic Hh; ShhN, Shh N terminus; SPR, surface plasmon resonance.

The Rockefeller University Press $30.00
J. Cell Biol. Vol. 192 No. 4 691–704
www.jcb.org/cgi/doi/10.1083/jcb.201008087

features of that glypican and on which growth factors and growth factor receptors are expressed by a specific cell type (Filmus et al., 2008).

Glypicans were first implicated in the regulation of Hh signaling by studies performed in *Drosophila*. Desbordes and Sanson (2003) and Lum et al. (2003) reported that Dlp (but not Dally) is required for optimal Hh signaling in a cell-autonomous manner. Epistatic experiments suggested that Dlp facilitates the interaction between Hh and its receptor Patched 1 (Ptc1) at the cell surface (Desbordes and Sanson, 2003). Our laboratory has recently provided experimental evidence of the involvement of a mammalian glypican in the regulation of Hh signaling. We showed that GPC3 acts as a negative regulator of Hh activity by competing with Ptc1 for Hh binding (Capurro et al., 2008, 2009).

There is strong genetic evidence indicating that the activation of the Hh signaling pathway plays a causal role in the progression of RMS. First, patients with the Gorlin syndrome, in which the Hh pathway is activated as a result of loss-of-function mutations of *Ptc1*, display a predisposition for RMS (Hahn et al., 1996; Gorlin, 2004). Second, *Ptc1* heterozygous mice frequently develop RMS (Hahn et al., 1998). Third, a proportion of informative RMSs show loss of heterozygosity in the *Ptc1* region (Bridge et al., 2000). In addition, the fact that many RMSs express Hh suggests that Hh signaling can be activated in an autocrine manner in these tumors (Tostar et al., 2006). The authors of the study that implicated GPC5 in the progression of RMS investigated the possibility that the growth-promoting effect of GPC5 was the result of the ability of this glypican to stimulate the activity of three heparan-binding growth factors: FGF, hepatocyte growth factor, or Wnt1 (Williamson et al., 2007). They observed that GPC5 induces a slight increase in the proliferation rate of an RMS cell line in the presence of each of these growth factors. However, the possibility that GPC5 activates Hh signaling in RMS was not investigated.

Given the fact that glypicans are known to regulate the Hh signaling pathway and that this signaling pathway plays a role in RMS, we hypothesized that GPC5 promotes RMS cell proliferation by stimulating endogenous Hh activity. In this paper, we present experimental evidence supporting this hypothesis. In addition, we uncover the molecular basis for the differential effect of GPC5 and GPC3 on the signaling activity of Hh.

Results

GPC5 stimulates Hh signaling in RMS cells

As a first approach to investigate whether GPC5 stimulates Hh signaling in RMS cells, we studied the effect of GPC5 knockdown on the expression of Gli1, a very well-characterized target of Hh signaling (Ruiz i Altaba et al., 2007). To this end, we used RH30, an RMS cell line that expresses high levels of GPC5 (Williamson et al., 2007) and Hh (unpublished data). To knock down GPC5 expression, cells were incubated with a commercially available GPC5 siRNA, which has already been used for this purpose (Williamson et al., 2007). Western blotting analysis showed that the expression of GPC5 in RH30 cells was strongly down-regulated by the targeting siRNA compared with cells

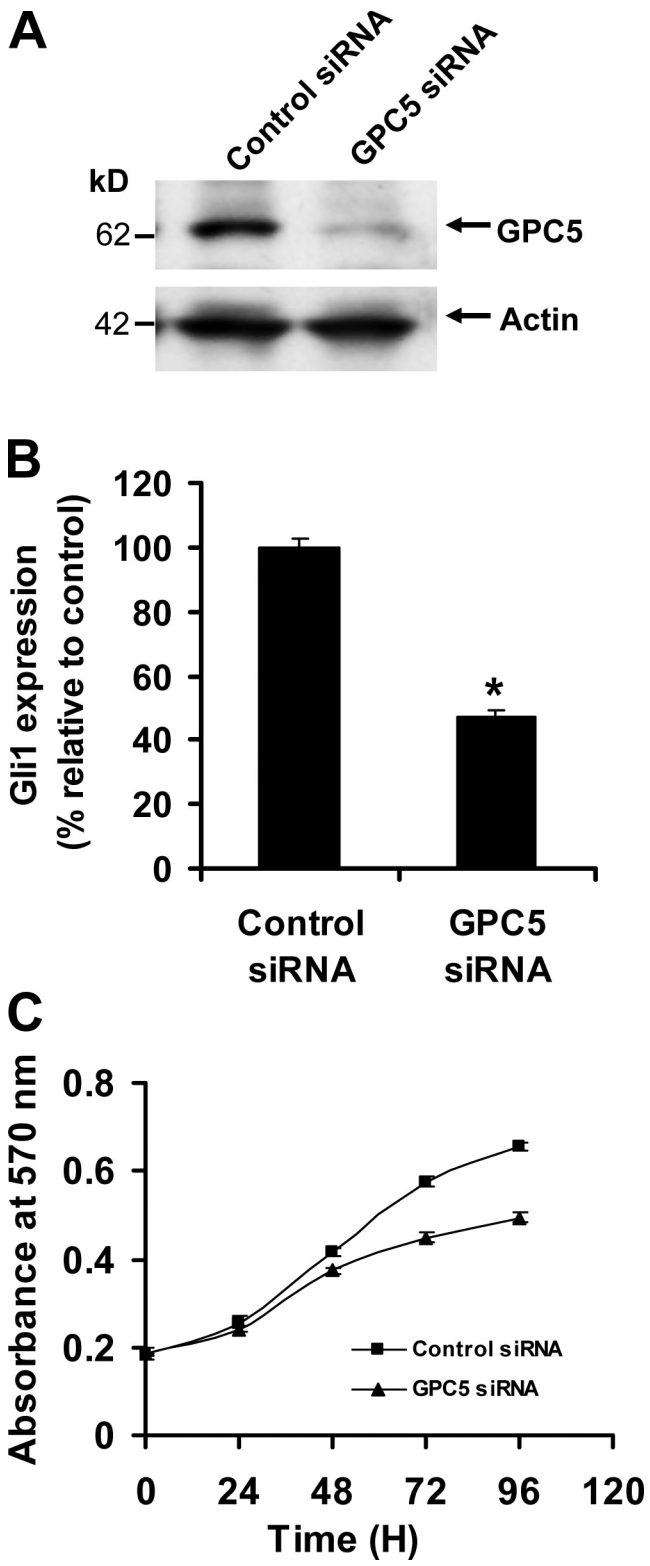

Figure 1. **GPC5 siRNA inhibits proliferation and Gli1 expression in RH30 RMS cells.** Cells were treated with the indicated siRNAs for 24 h. (A) Western blot analysis. 2 d after the removal of the siRNA, cells were lysed, and levels of GPC5 were assessed by Western blot analysis. Actin was used as a loading control. (B) Real-time RT-PCR. Quantitative analysis of Gli1 expression using real-time PCR was performed. Error bars represent the means of three independent measurements ± SD. The asterisk indicates a significant difference from the control ($P < 0.01$). (C) MTT assays were performed at the indicated time points. Results represent the means of quintuplicates ± SD. The experiment was performed three times with similar results.

treated with nontargeting siRNA control (Fig. 1 A). It is well established that most cells that produce high levels of glypicans display a proportion of these proteins in a nonglycanated form. In this regard, it should be noted that the commercially available anti-GPC5 antibody that was used in this study has very low sensitivity for the detection of glycanated GPC5. In fact, most antiglypican antibodies fail to detect the glycanated endogenous glypicans in Western blots, probably because the GAG chains block epitope recognition on the blotted membrane (Saunders et al., 1997; Veugelers et al., 1999). Thus, the Western blot in Fig. 1 A only shows the 65-kD GPC5 core protein. However, the glycanated form could be detected when high amounts of purified GPC5 were submitted to Western blot analysis (see Fig. 3 B, top right). The levels of Gli1 in the RH30 cells treated with the GPC5 siRNA or siRNA control were measured by real-time RT-PCR. We found that, compared with the control siRNA, the GPC5 siRNA significantly down-regulated Gli1 levels (Fig. 1 B). As previously shown by Williamson et al. (2007), we also observed that down-regulation of GPC5 significantly inhibits the proliferation rate of the RMS cells (Fig. 1 C).

As an additional approach to investigate the impact of GPC5 on Hh activity in RMS cells, we assessed the effect of ectopic GPC5 on Hh signaling in CW9019, an RMS cell line that expresses low levels of GPC5, similar to normal muscle (Williamson et al., 2007) and Hh (unpublished data). To this end, CW9019 cells were transfected with a GPC5 expression vector or vector alone, and GPC5-overexpressing cells were sorted by FACS. Overexpression of GPC5 in the sorted cells was verified by Western blot analysis (Fig. 2 A). Ectopic GPC5 induced a significant increase in Gli1 expression (Fig. 2 B). Consistent with this observation, the GPC5-transfected CW9019 cells proliferated faster than the vector-transfected cells (Fig. 2 C). Significantly, the GPC5-induced stimulation of cell proliferation was completely abrogated by cyclopamine, a well-characterized inhibitor of Hh signaling (Fig. 2 C). It should be noted that cyclopamine also inhibited the proliferation of vector control–transfected cells, suggesting that the Hh signaling pathway already displays a significant degree of activation in the CW9019 cells, probably as a result of an autocrine loop. Collectively, these experiments indicate that GPC5 stimulates cell proliferation in RMS cells by activating Hh signaling.

We also investigated the effect of GPC5 on Hh signaling by using a luciferase reporter assay, in which luciferase expression is driven by an Hh-responsive promoter. Because this reporter assay does not work in RMS cells (unpublished data), we used C2C12 myoblasts that, like RMS cells, are the result of the malignant transformation of immature muscle cells. As shown in Fig. 3 A, the transient expression of GPC5 in C2C12 cells stimulated in a dose-dependent manner the luciferase activity induced by Sonic Hh (Shh) N terminus (ShhN)–containing conditioned medium. This result provides additional support to the hypothesis that GPC5 stimulates Hh signaling.

Next, we studied the role of the GAG chains in the GPC5-induced stimulation of Hh signaling. To this end, we generated a GPC5 mutant that cannot be glycanated because of the mutation of the five insertion sites for the GAG chains (GPC5ΔGAG). The expression of this mutant was verified by Western blot analysis

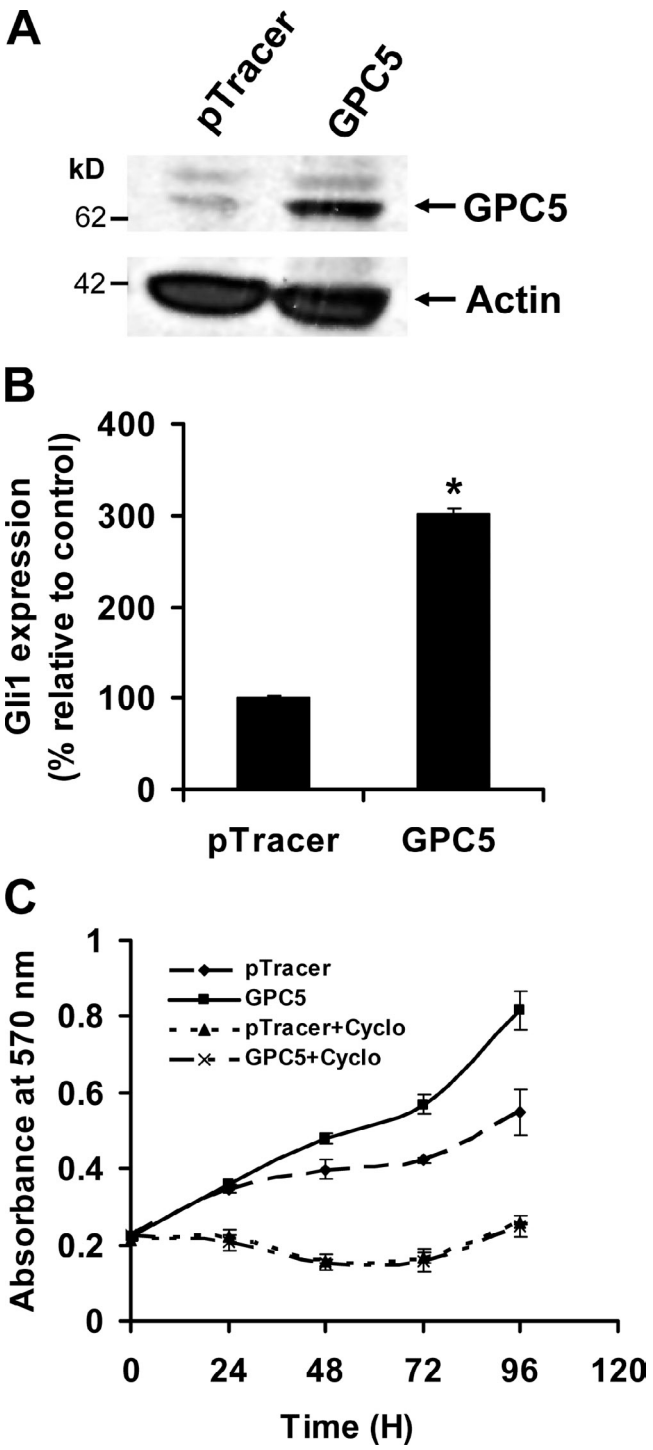

Figure 2. **GPC5 overexpression stimulates proliferation and Gli1 expression in CW9019 RMS cells.** Cells were transfected with GPC5 or control vector (pTracer). (A) Western blot analysis of GPC5 expression. Actin was used as a loading control. (B) Quantitative analysis of Gli1 expression using real-time RT-PCR. Error bars represent the means of three independent measurements ± SD. The asterisk indicates a significant difference from the control ($P < 0.01$). (C) MTT assays were performed at the indicated time points. Media were replaced every 24 h. Results represent the means ± SEM of quintuplicates. The experiment was repeated twice with similar results. Cyclo, cyclopamine.

of transiently transfected 293T cells. As shown in Fig. 3 B (top left), the GPC5ΔGAG mutant generated a band corresponding to the core protein that was significantly stronger than that

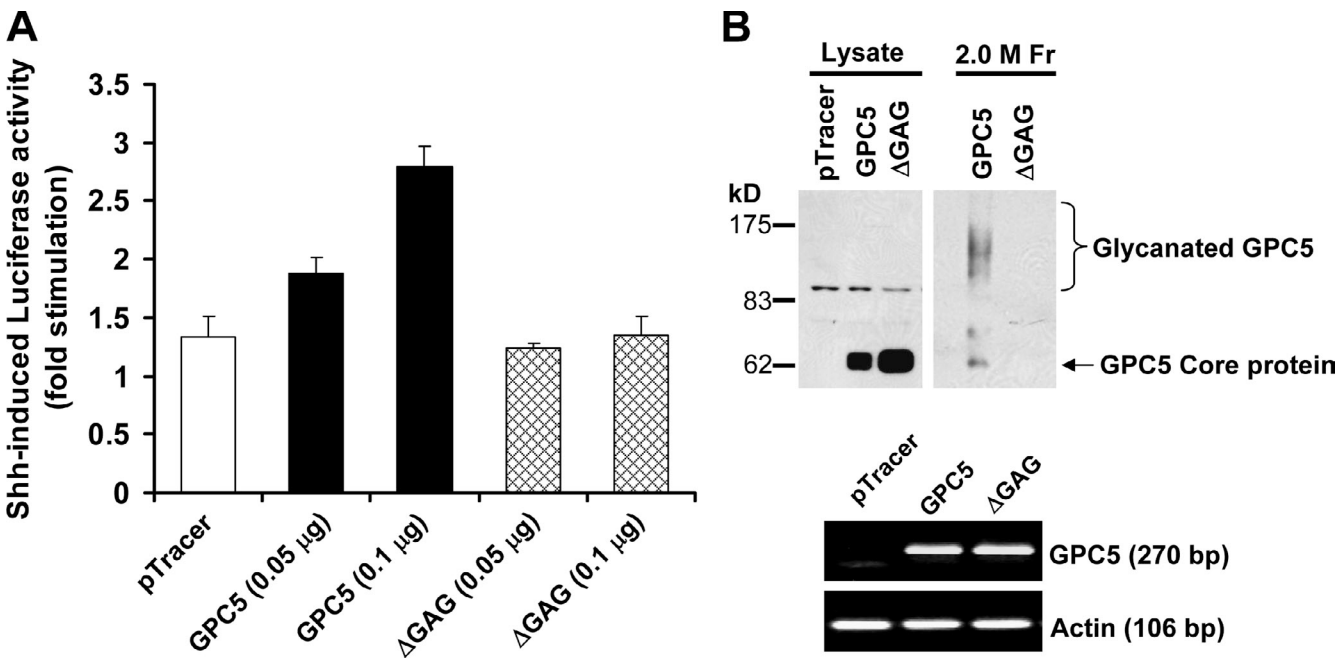

Figure 3. **GPC5 stimulates Shh-induced signaling.** (A) Hh reporter assay. Mouse myoblast C2C12 cells were transfected with the indicated vectors along with a luciferase reporter and β-galactosidase. An Hh reporter assay was then performed. Bars represent normalized fold stimulation of luciferase activity induced by ShhN (means ± SD of triplicates). The experiment was repeated three times with similar results. (B) Transient expression of GPC5 and GPC5ΔGAG (ΔGAG). 293T cells were transiently transfected with the indicated vectors. 2 d after transfection, the expression of the GPC5 variants was assessed by Western blot analysis of whole cell lysates (top left), the DEAE-purified material from the lysates (top right), or by RT-PCR (bottom). (top) Numbers on the left represent molecular mass markers. Actin was used as a control of the amount of RNA. Fr, fraction.

corresponding to wild-type GPC5, despite the fact that the transfected cells produced similar levels of the respective transcripts (Fig. 3 B, bottom). This is most likely because a large proportion of the wild-type GPC5 is glycanated and because the glycanated form cannot be detected in the Western blot as a result of the low sensitivity of the antibody. To verify this, we concentrated the glycanated GPC5 from the lysates of transfected cells by anion-exchange chromatography, and the concentrated material was submitted to Western blot analysis. The glycanated GPC5 could then be detected as a high molecular mass smear (Fig. 3 B, top right). As expected, no signal was detected in the material purified in the same way from the lysates of the cells transfected with the GPC5ΔGAG mutant because this mutant does not bind to the DEAE-Sepharose.

We also studied the effect of GPC5ΔGAG on Hh signaling by using the same Hh reporter assay as used for wild-type GPC5. As shown in Fig. 3 A, the nonglycanated GPC5 did not stimulate Hh signaling, indicating that the GAG chains are essential for the GPC5-induced stimulation of this signaling pathway.

GPC5 promotes the binding of Shh to Ptc1

Next, we investigated the mechanism by which GPC5 stimulates Hh signaling in RMS cells. Based on the experiments in *Drosophila* that showed that Dlp promotes Hh activity by acting upstream or at the level of Ptc1 (Desbordes and Sanson, 2003), we hypothesized that GPC5 can stimulate the interaction between Hh and Ptc1. To test this hypothesis, we transiently transfected GPC5 into 293T cells. 2 d after transfection, cells were incubated with an Shh-AP fusion protein for 2.5 h at 4°C. After removing the unbound material, cells were washed and lysed, and Ptc1 was immunoprecipitated. The amount of Shh bound to the immunoprecipitated Ptc1 was quantified by measuring the AP activity in the precipitate. As shown in Fig. 4, we found that GPC5 significantly stimulates, in a dose-dependent manner, the binding of Shh to Ptc1. It should be noted that, unlike the Hh that is produced endogenously by the RMS cells, the Shh-AP fusion protein is in a monomeric form. However, we have demonstrated that GPC5 stimulates the signaling of both the monomeric and oligomeric forms of Shh (Fig. S1).

We also studied the effect of the GPC5ΔGAG mutant on the binding of Shh to Ptc1 following the same protocol as described for the wild-type GPC5. We found that GPC5ΔGAG cannot stimulate this binding (Fig. 4). This is consistent with the result of the Hh reporter assay showing that the nonglycanated GPC5 cannot stimulate Hh signaling (Fig. 3 A).

GPC5 binds to Shh

Next, we investigated the mechanism by which GPC5 stimulates the binding of Hh to Ptc1. We hypothesized that GPC5 can facilitate/stabilize the interaction of Hh with Ptc1. If this hypothesis were correct, it would be expected that GPC5 interacts with both Hh and Ptc1. Our laboratory has already demonstrated that Shh binds to GPC3 with high affinity (Capurro et al., 2008). First, we investigated whether GPC5 interacts with Shh. As an initial approach, we performed surface plasmon resonance (SPR) analysis. To this end, a GPC5-AP fusion protein was purified from 293T cells and attached to a Biacore sensor chip. The analysis showed that Shh binds to GPC5-AP with a K_d of 310 ± 60 nM (Fig. 5 A, top; and Table S1). We also performed

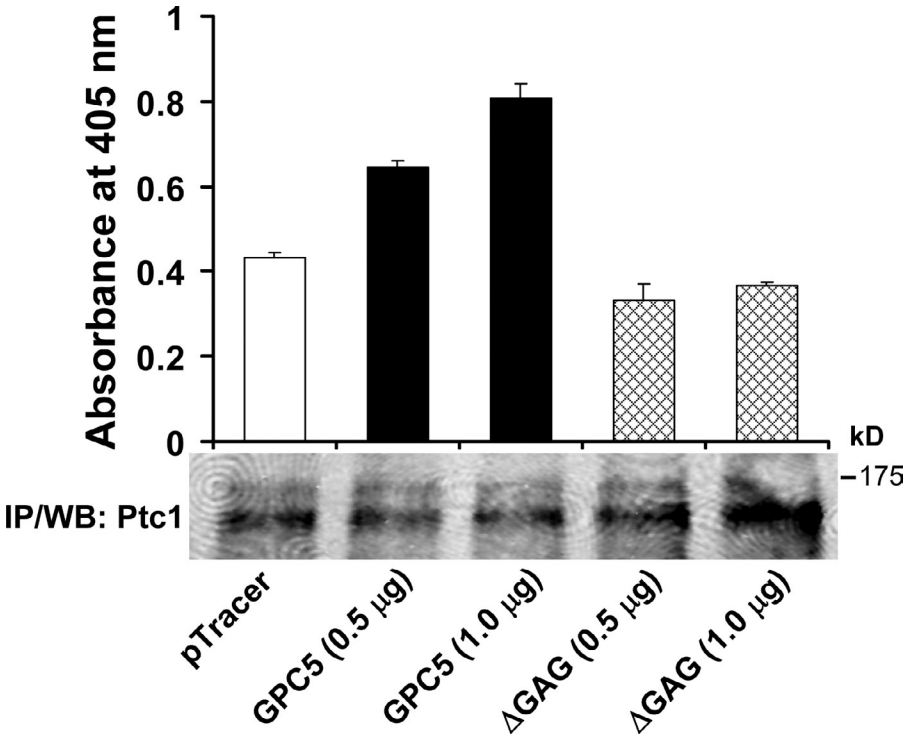

Figure 4. **GPC5 promotes Shh binding to Ptc1.** 293T cells were transiently transfected with increasing amounts of the indicated expression vectors or empty vector (pTracer). 48 h after transfection, the cells were incubated with Shh-AP or AP at 4°C for 2.5 h. After washing, endogenous Ptc1 was immunoprecipitated (IP), and the amount of Shh-AP bound to the immunoprecipitated Ptc1 was determined by measuring AP activity. Bars represent the relative amount of Shh-AP bound to Ptc1 after subtraction of the binding measured for AP alone (means ± SD of triplicates). The corresponding immunoprecipitated Ptc1 from each sample was assessed by Western blot (WB) analysis (bottom).

SPR analysis of the interaction of Shh with GPC5-AP purified from the RH30 RMS cell line. In this case, the calculated K_d was 1,530 ± 625 nM (unpublished data). Notably, the affinity of the GPC5–Shh interactions is significantly lower than that of the interaction between GPC3 and Shh. Previously, we have shown that the high affinity interaction of Shh with GPC3 is mediated by the core protein (Capurro et al., 2008). However, when the GAG chains of GPC5-AP were removed by digestion with GAG-degrading enzymes, the binding of Shh to GPC5-AP was dramatically inhibited (Fig. 5 A, bottom), indicating that the GAG chains play a key role in the binding. We also investigated the interaction between GPC5 and Shh in the context of intact cells. To this end, 293T cells were transiently transfected with GPC5 or GPC5ΔGAG, and the transfected cells were incubated with an Shh-AP fusion protein. Unbound material was removed, cells were washed and lysed, and GPC5 or GPC5ΔGAG was immunoprecipitated. The level of AP activity in the immunoprecipitates was then measured. Immunoprecipitates from cells transfected with vector alone were used as negative controls. We found significant binding of Shh-AP to wild-type GPC5, but the binding of Shh to the nonglycanated mutant (ΔGAG) was significantly lower than that of the wild-type GPC5 (Fig. 5 B). Collectively, the SPR analysis and binding experiments indicate that GPC5 binds to Shh mainly through the GAG chains.

GPC5 binds to Ptc1

As an initial approach to investigate the interaction of GPC5 with Ptc1, we performed a coimmunoprecipitation assay. Expression vectors for Ptc1 and for wild-type GPC5 or GPC5ΔGAG were transiently transfected into 293T cells. Cells were then lysed, GPC5 or GPC5ΔGAG was immunoprecipitated, and the presence of Ptc1 in the precipitated material was assessed by Western blot analysis. We found that Ptc1 coimmunoprecipitated with wild-type GPC5 but not with GPC5ΔGAG (Fig. 6 A). Next, we studied the GPC5–Ptc1 interaction by performing a cell-binding assay. Ptc1- or control vector–transfected 293T cells were incubated with conditioned media containing equal concentrations of a GPC5-AP fusion protein or a GPC5ΔGAG-AP fusion protein at 4°C for 2 h. After washing with cold PBS, cells were lysed, and the cell-bound AP activity was measured. As shown in Fig. 6 B, we found that the binding of GPC5-AP to the Ptc1-transfected cells is much higher than that to the vector control–transfected cells. Consistent with the coimmunoprecipitation results, GPC5ΔGAG-AP did not bind to the Ptc1-transfected cells. We also studied the interaction between GPC5 and Ptc1 by a pull-down assay. To this end, 293T cells were transiently transfected with an expression vector for HA (hemagglutinin-A)-tagged Ptc1, cells were lysed, and the lysate was mixed with beads covered with an anti-HA antibody. The beads were then incubated with conditioned media containing equal concentrations of a GPC5-AP fusion protein or a GPC5ΔGAG-AP fusion protein. After washing, the amount of AP that remained bound to the beads was measured. We found that although there was a significant binding of wild-type GPC5 to the beads, the GPC5ΔGAG mutant did not show any detectable binding (Fig. 6 C). This result is consistent with the result of the coimmunoprecipitation. Next, we tried to estimate the affinity of the GPC5–Ptc1 interaction by performing the pull-down assay with various concentrations of GPC5-AP. To measure the concentration of GPC5-AP in the conditioned media, we performed a comparative Western blot using different amounts of purified GPC5ΔGAG (unpublished data). The Scatchard analysis showed that GPC5 interacts with Ptc1 with a K_d of 37 nM (Fig. 6 D). From these experiments, we conclude that

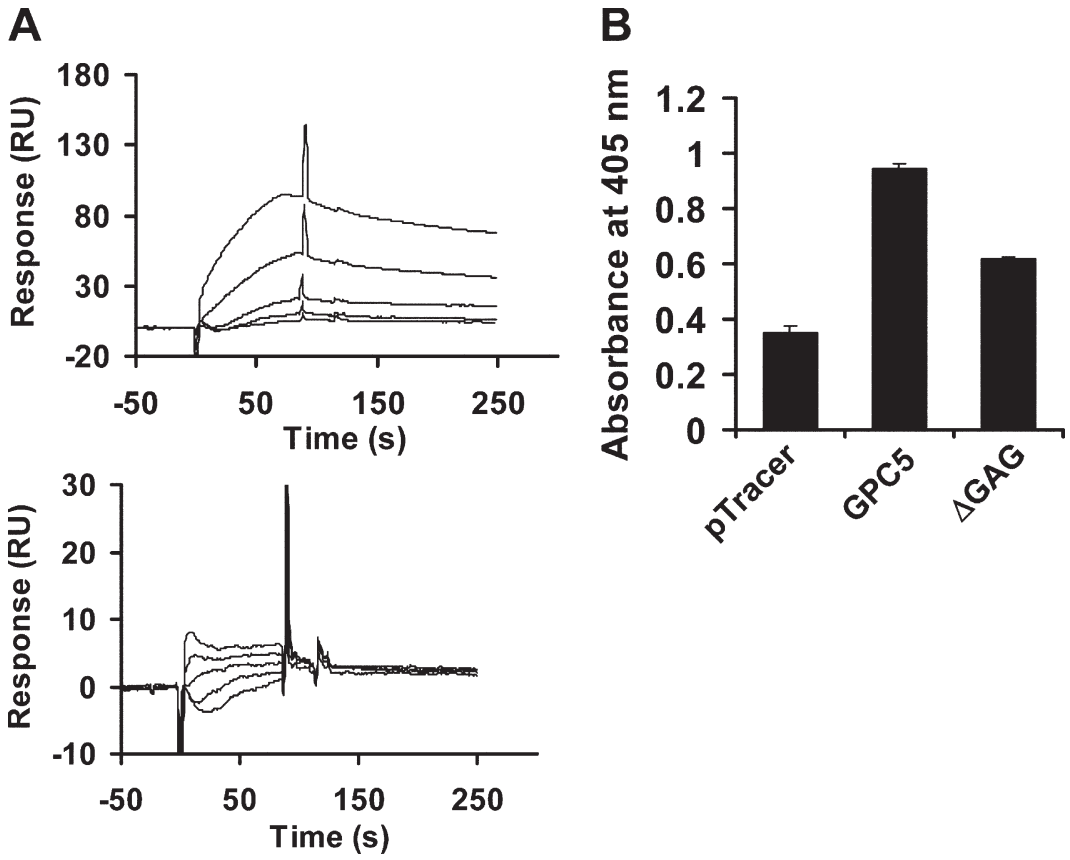

Figure 5. **Shh binds to GPC5.** (A) SPR analysis of the GPC5–Shh interaction. Various concentrations of Shh (bottom to top: 112.5, 225, 450, 900, and 1,800 nM) were used for the interaction assay with GPC5-AP (top) or deglycanated GPC5-AP (bottom). *n* = 1. (B) Binding of Shh-AP to GPC5-transfected 293T cells. Cells were transfected with GPC5, GPC5ΔGAG (ΔGAG), or control vector (pTracer) and were incubated with Shh-AP or AP alone at 4°C for 2 h. Cells were lysed, GPC5 was immunoprecipitated, and the AP activity in the precipitate was measured. Bars represent the relative amounts of Shh-AP bound to GPC5 after subtraction of the binding measured for AP alone (means ± SD of duplicates). RU, response unit.

GPC5 binds to Ptc1 with high affinity and that the GAG chains are essential for this interaction.

GPC5 can be found in the ciliary membrane

Recent studies have shown that the primary cilium is required to trigger Hh signaling and that the interaction of Hh with Ptc1 occurs at the ciliary membrane (Rohatgi et al., 2007; Kiprilov et al., 2008; Milenkovic et al., 2009). We decided therefore to investigate whether GPC5 can also be found at the ciliary membrane. To this end, NIH 3T3 cells were transfected with GPC5 or GPC5ΔGAG and stained with antibodies against GPC5 and acetylated tubulin, a marker of primary cilia. As shown in Fig. 7 A, the GPC5 antibody strongly stained the primary cilium. In contrast, a very low level of staining was observed in GPC5ΔGAG-transfected cells. Quantification of the cilia-specific immunofluorescence confirmed the differential localization of GPC5 and the nonglycanated mutant (Fig. 7 B). We also investigated whether GPC3 can be found in cilia. As shown in Fig. 7 C, we could not detect any staining in cilia of GPC3-transfected NIH 3T3 cells. We also investigated the localization of endogenous GPC5 by staining the RMS cell line RH30. Although primary cilia are difficult to detect in rapidly growing RH30 cells, a low proportion of cilium-carrying cells could be detected after serum starvation for 48 h. As shown in Fig. 7 D, the GPC5 antibody strongly stained the primary cilia of RH30 cells.

The binding of GPC5 to Ptc1 is mediated by both HS and CS

We have previously shown that GPC3 does not bind to Ptc1 (Capurro et al., 2008). Thus, the results shown in Fig. 6 demonstrating that GPC5 binds to Ptc1 through its GAG chains strongly suggest that the differential binding of these two glypicans is caused by differences in the GAG chains. Because it has been previously shown that, unlike GPC3, which only displays HS chains (Filmus et al., 1995), GPC5 also carries CS chains (Saunders et al., 1997), we decided to study whether the binding of GPC5 to Ptc1 is mediated by the CS chains. First, we tried to confirm that endogenous GPC5 from RMS cells carries CS chains. To this end, we partially purified GPC5 from RH30 cells by anion-exchange chromatography. Aliquots of the purified material were then digested with heparitinase (HSase) II, which specifically cleaves HS chains, or chondroitinase (CSase) ABC, which specifically cleaves CS chains. We also digested another aliquot with both enzymes together. The digested material was then analyzed by Western blotting with an anti-GPC5 antibody. Fig. 8 A shows that no bands or smears were seen in the undigested material. This is expected given the fact that the anti-GPC5 antibody has low sensitivity for the glycanated GPC5, and the GPC5 core protein does not bind to the DEAE-Sepharose. On the other hand, a single band corresponding to the GPC5

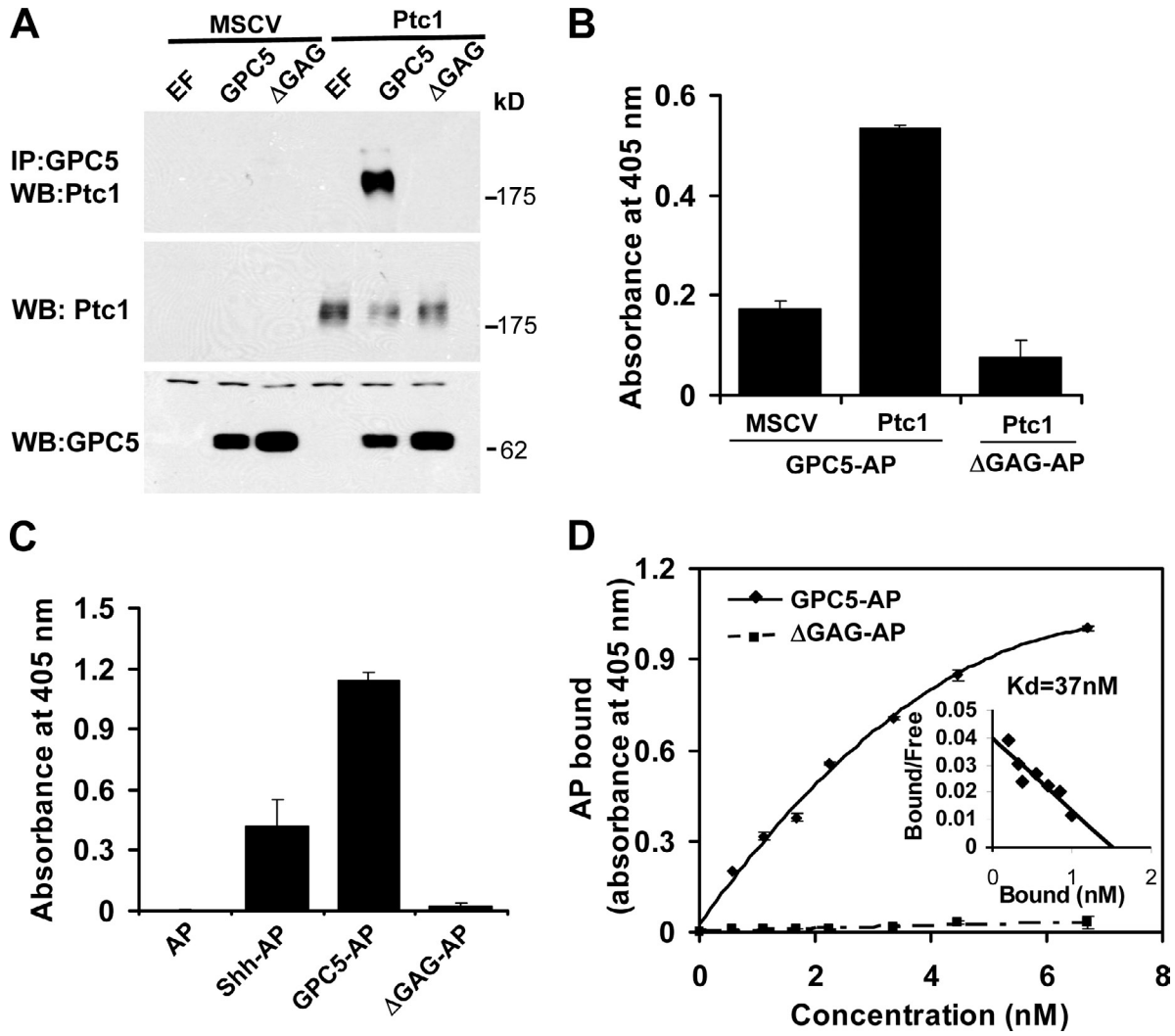

Figure 6. **Ptc1 binds to GPC5.** (A) Coimmunoprecipitation. 293T cells were transfected with the indicated plasmids, and GPC5 was immunoprecipitated (IP). The presence of Ptc1 in the precipitated material was then assessed by Western blotting (WB; top). The expression levels of Ptc1 (middle) and GPC5 (bottom) in the transfected cells were verified by Western blotting. Murine stem cell virus (MSCV) and elongation factor (EF) indicate expression vectors alone. (B) Cell-binding assay. 293T cells were transfected with Ptc1 or control vector (murine stem cell virus) and were incubated with GPC5-AP, GPC5ΔGAG-AP (ΔGAG-AP), or AP alone at 4°C for 2 h. Cells were then lysed, and the AP activity of aliquots of cell lysates containing the same amount of protein was measured. Bars represent the relative amount of GPC5-AP bound to Ptc1 after subtraction of the binding measured for AP alone. (C) Pull-down assay. Interactions of Ptc1 with Shh-AP (positive control), GPC5-AP, GPC5ΔGAG-AP, or AP only were investigated using a pull-down assay. The experiment was repeated twice with similar results. (D) Affinity measurement. The affinity of the interaction between Ptc1 and GPC5-AP was measured using a binding assay. The binding data were analyzed by Scatchard plotting (inset). Error bars represent the means of duplicates ± SD.

core protein was detected after digestion with HSase, suggesting that a proportion of GPC5 in RMS cells only displays HS. No bands or smears were seen after digestion with CSase, indicating that most or all GPC5 from RMS cells display HS chains. The digestion with both enzymes generated a band corresponding to the core protein that was significantly more intense than that generated after digestion with HSase alone, indicating that a significant proportion of GPC5 in RMS cells carries both HS and CS.

To investigate the role of the CS chains in the binding of GPC5 to Ptc1, relatively large amounts of purified GPC5 are required. To facilitate the purification of larger quantities of GPC5, we transiently transfected RMS cells with an expression vector for a GPC5-AP fusion protein, which is secreted to the conditioned medium. GPC5-AP was purified from the medium by anion-exchange chromatography and affinity chromatography and was submitted to treatment with HSase, CSase, or both enzymes to confirm that the fusion protein carries a proportion of CS and HS that is similar to that of the endogenous GPC5. The digested material was analyzed by Western blotting. This analysis showed that, like the endogenous GPC5, most of the purified GPC5-AP fusion protein carries both HS and CS (Fig. 8 B). It should also be noted that the smear corresponding to the glycanated GPC5-AP could be detected by the anti-GPC5 antibody. This suggests that there might be some differential accessibility to the epitope recognized by the anti-GPC5 antibody in the wild-type GPC5 purified from cell lysates compared with the GPC5-AP purified from conditioned media. This is probably because GPC5-AP has been separated from other proteoglycans by the affinity chromatography, and the epitope

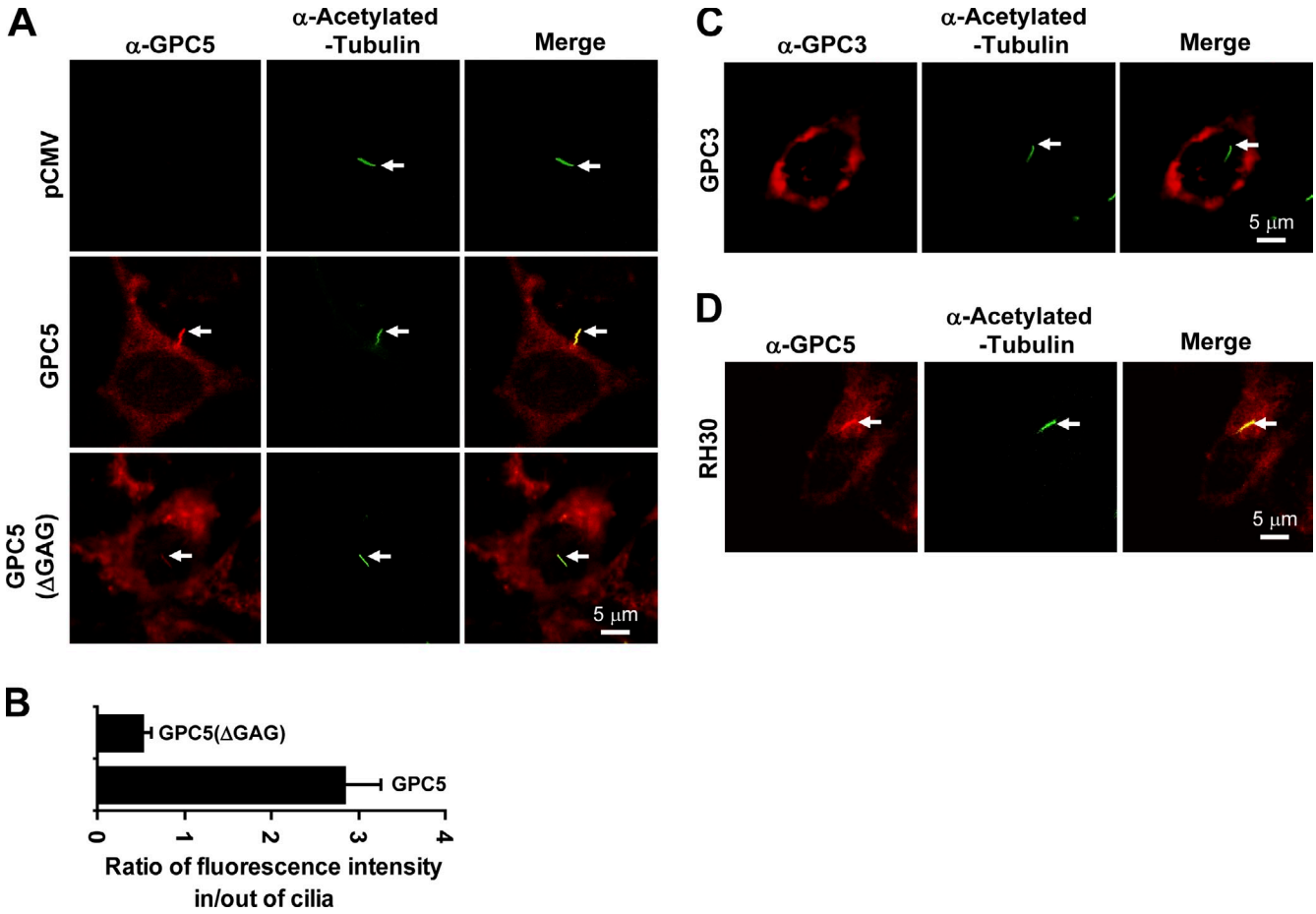

Figure 7. **GPC5 localizes to the primary cilium.** (A) NIH 3T3 cells transfected with the indicated vectors were stained with the indicated antibodies. (B) Ratio of fluorescence intensity in/out of cilia of NIH 3T3 cells transfected with GPC5 or GPC5ΔGAG. Error bars represent the means of seven cells ± SD. (C) NIH 3T3 cells transfected with GPC3 were stained with the indicated antibodies. (D) Immunofluorescence of endogenous GPC5 in the RMS cell line RH30. In the merged pictures, yellow indicates a colocalization of GPC5 with cilia. Cilium is indicated by arrows.

recognized by the anti-GPC5 is more accessible in the Western blot membrane.

To investigate the role of the HS and CS chains in the binding of GPC5 to Ptc1, aliquots of the GPC5-AP fusion protein were digested with HSase, CSase, or both enzymes together, and a pull-down assay was performed with undigested and digested fusion protein. We found that the digestion of the HS chains strongly inhibited the binding of GPC5-AP to Ptc1. The effect of CSase was significantly less pronounced (Fig. 8 C). Consistent with this result, we found that the binding of GPC5-AP to Ptc1 is strongly inhibited by heparan but partially reduced by CS-A from bovine trachea (Sigma-Aldrich), which mostly contains the monosulfated disaccharide GlcAβ1–3GaINAc(4-*O*-sulfate), the main component of mammalian CS (Fig. 8 D). Interestingly, the binding of GPC5-AP to Ptc1 was strongly inhibited by the highly sulfated CS-E from squid cartilage, containing >60% of GlcAβ1–3GaINAc(4,6-*O*-disulfate), which is not normally found in mammals (Sugahara et al., 2003). These data suggest that sulfation plays an important role in the binding of the GAG chains of GPC5 to Ptc1. Collectively, our results indicate that the binding of GPC5 to Ptc1 is mostly mediated by the HS chains and that the CS chains contribute to the binding when the HS chains are present.

The HS chains of GPC5 display a higher degree of sulfation than those of GPC3

It is well established that the binding specificity of the HS chains is predominantly determined by the degree and type of sulfation (Bishop et al., 2007; Gorsi and Stringer, 2007). Thus, the fact that the binding of GPC5 to Ptc1 is mostly mediated by the HS chains and that, unlike GPC5, GPC3 does not bind to Ptc1 (Capurro et al., 2008) strongly suggests that the HS chains of GPC5 display a different sulfation pattern than those of GPC3. We decided, therefore, to compare the sulfation profile of these two glypicans. The degree of sulfation of GAG chains produced by a given cell type is determined, at least in part, by the levels of sulfotransferases and sulfatases expressed by this cell type (Gorsi and Stringer, 2007). In this regard, it should be noted that, so far, the GPC5 and GPC3 that we used to establish the differential binding to Ptc1 were produced in different cell types: GPC3 was purified from transfected 293T cells (Capurro et al., 2008), and GPC5 was purified from RMS cells (this study). We considered, therefore, that it was important to compare the sulfation of the HS chains from GPC3 and GPC5 that were expressed in the same cell type. Because GPC3 is not expressed by RMS cells, we decided to compare GPC5 and GPC3 produced in NIH 3T3 cells. We have previously used these cells

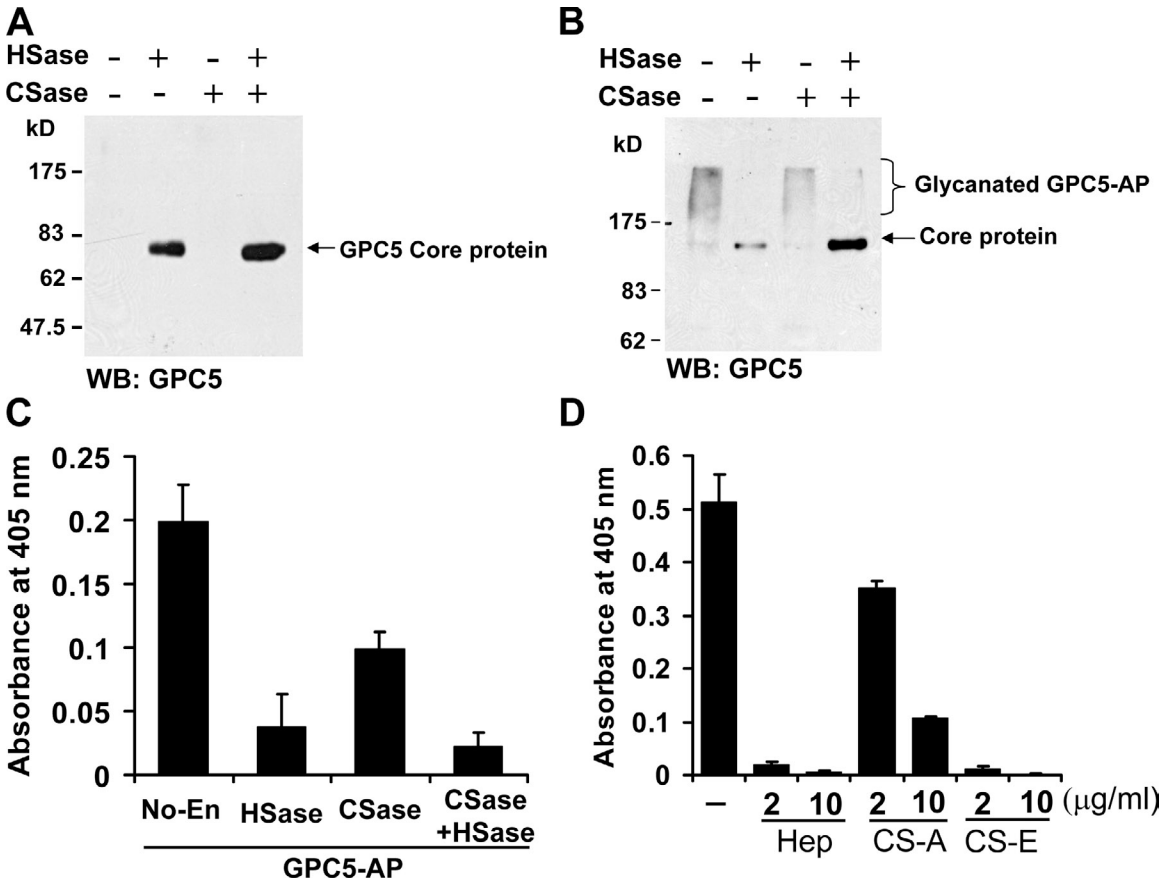

Figure 8. **GPC5 binds to Ptc1 through its GAG chains.** (A) Analysis of the GAG chains of GPC5. Endogenous GPC5 was partially purified from RH30 cells using a DEAE-Sepharose column, digested with heparitinase II (HSase), chondroitinase ABC (CSase), or both enzymes together, and the digests were submitted to Western blot (WB) analysis. (B) Analysis of the GAG chains of GPC5-AP. GPC5-AP was purified from transiently transfected RH30 cells. The purified GPC5 was digested with the indicated enzymes, and the digests were submitted to Western blot analysis. (C) GPC5-AP–Ptc1-binding assay. An aliquot of each sample from B was used to perform a pull-down assay as described in Fig. 6 C. The experiment was repeated twice with similar results. No-En, no enzyme (undigested GPC5-AP). (D) Effect of various GAGs on GPC5–Ptc1 binding. A pull-down assay with undigested GPC5 was performed in the presence of the indicated concentrations of heparan (Hep), chondroitin sulfate A (CS-A), or chondroitin sulfate E (CS-E). Error bars represent means of duplicates ± SD.

to show that GPC3 inhibits Hh signaling (Capurro et al., 2008). We first investigated whether, like in RMS cells, GPC5 stimulates Hh signaling in NIH 3T3 cells. To this end, we performed an Hh reporter assay. We found that GPC5 strongly stimulates, in a dose-dependent manner, Hh signaling (Fig. 9 A). As a control, we verified that in the same experimental conditions GPC3 inhibits Hh signaling. In addition, we tested the effect of the GPC5ΔGAG mutant in the reporter assay. As we showed for C2C12 cells, we observed that this mutant does not stimulate Hh signaling in NIH 3T3 cells (Fig. 9 A). Next, we investigated whether GPC3 and GPC5 produced in NIH 3T3 display a similar type of GAG chains as the cells that were previously used to demonstrate the differential binding of these two glypicans to Ptc1. To this end, NIH 3T3 cells were transiently transfected with the GPC5-AP and GPC3-AP fusion proteins. These proteins were then purified from the transfected cells as described in Materials and methods and were digested with HSase, CSase, or both enzymes together. The digested products were then analyzed by Western blotting. As shown in Fig. 9 B, we found that, as previously observed in other cell types, GPC3 displays HS chains, and GPC5 displays a mixture of both HS and CS. We then compared the binding of the two fusion proteins to Ptc1 by a pull-down assay. We found that GPC5-AP purified from NIH 3T3 cells displays a much higher capacity to bind Ptc1 than GPC3-AP (Fig. 9 C). Furthermore, as we showed for the RH30 cells, we found that most of the binding of GPC5-AP to Ptc1 is mediated by the HS chains and that the CS chains contribute to the binding when the HS chains are present (Fig. 9 D).

Having shown that GPC5 and GPC3 expressed in NIH 3T3 cells display differential binding to Ptc1, we compared the sulfation profile of the HS chains from both glypicans in these cells. To this end, the purified glypicans were digested with a mixture of HSase I and III. The disaccharides generated by this digestion were labeled with 2-aminobenzamide (2AB) and separated by anion-exchange HPLC. The identity of each peak was confirmed by comparing the position of the eluted peaks with 2AB-labeled standard HS disaccharides (Fig. 9 E). The quantification of the disaccharides is shown in Fig. 9 F. According to the chromatogram, the HS of both GPC3-AP and GPC5-AP contain ΔHexUA-GlcNAc, ΔHexUA-GlcN(2-*N*-sulfate), ΔHexUA-GlcNAc(6-*O*-sulfate), ΔHexUA-GlcN(2-*N*-,6-*O*-disulfate), ΔHexUA(2-*O*-sulfate)-GlcN(2-*N*-sulfate),

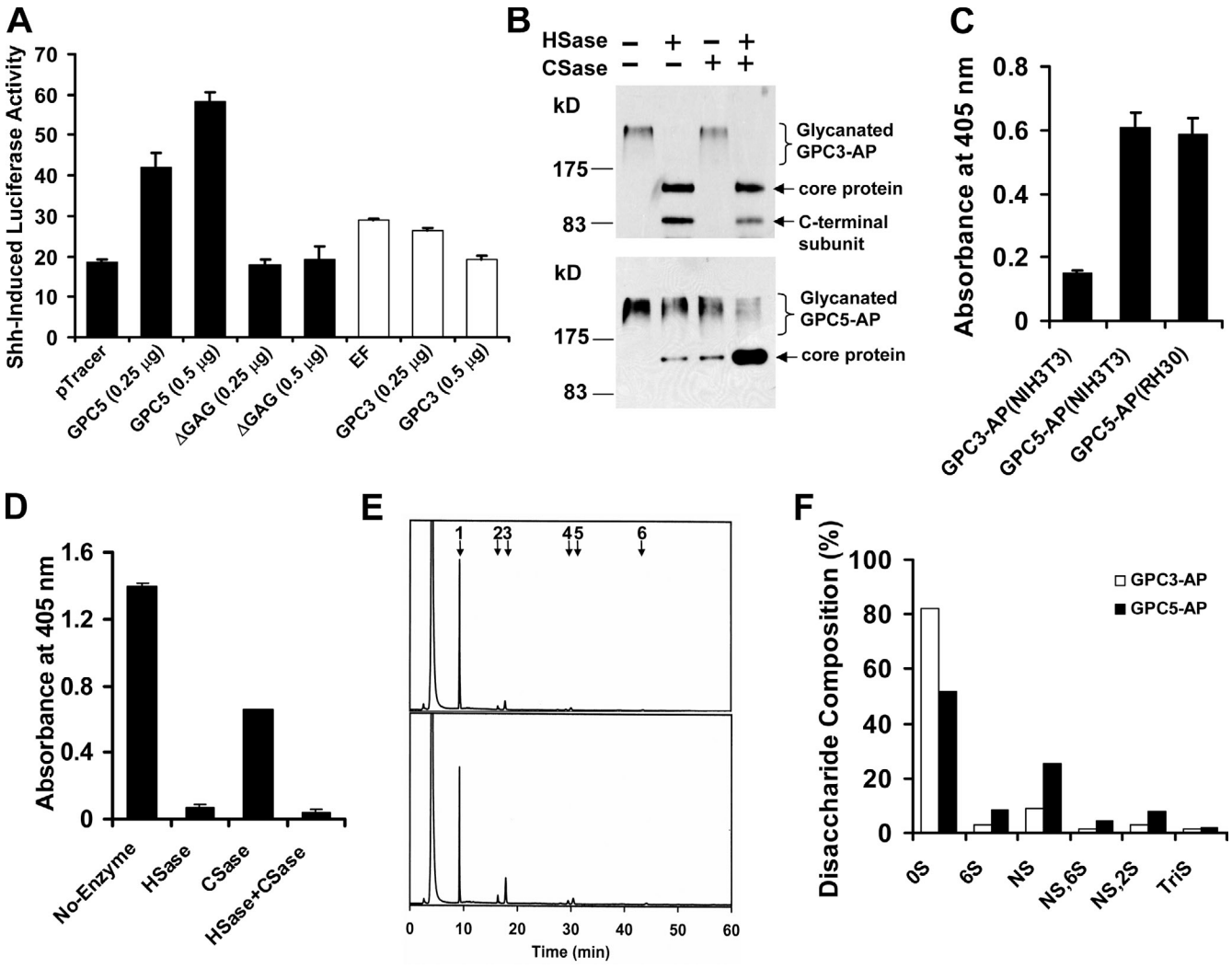

Figure 9. **The HS chains of GPC5 are more sulfated than those of GPC3.** (A) Hh reporter assay. NIH 3T3 cells were transfected with the indicated expression vectors or empty vectors (pTracer and elongation factor [EF]), and a transient luciferase reporter assay was performed as described in Fig. 3 A. Results represent the means ± SD of triplicates. (B) Analysis of the GAG chains. GPC3-AP or GPC5-AP was purified from transiently transfected NIH 3T3 cells, digested with the indicated enzymes, and analyzed by Western blotting. (C) Comparative binding of GPC3 or GPC5 to Ptc1. GPC3-AP or GPC5-AP were purified from the indicated transiently transfected cells, and their binding to Ptc1 was assessed by a pull-down assay. Error bars represent the means of duplicates ± SD. The experiment was repeated twice with similar results. (D) The role of the GAG chains of GPC5 from NIH 3T3 cells in its binding to Ptc1. GPC5-AP purified from NIH 3T3 cells was digested with the indicated enzymes, and the binding of the digested GPC5 samples to Ptc1 was assessed by a pull-down assay as described in Fig. 6 C. Error bars represent the means of duplicates ± SD. The experiment was repeated twice with similar results. (E) Disaccharide analysis of the HS chains. Purified GPC3-AP (top) and GPC5-AP (bottom) were digested with HSases, and the digested material was analyzed by HPLC. The elution positions of authentic 2AB disaccharide standards derived from HS are indicated by numbered arrows (top): (1) ΔHexUA-GlcNAc (0S), (2) ΔHexUA-GlcNAc(6-*O*-sulfate) (6S), (3) ΔHexUA-GlcN(2-*N*-sulfate) (NS), (4) ΔHexUA-GlcN(2-*N*-,6-*O*-disulfate) (NS,6S), (5) ΔHexUA(2-*O*-sulfate)-GlcN(2-*N*-sulfate) (NS,2S), and (6) ΔHexUA(2-*O*-sulfate)-GlcN(2-*N*-,6-*O*-disulfate) (TriS). (F) Bar graph displaying the results of the disaccharide analysis. $n = 1$.

and ΔHexUA(2-*O*-sulfate)-GlcN(2-*N*-,6-*O*-disulfate) in varying proportions (ΔHexUA represents 4-deoxy-L-threohex-4-enepyranosyluronic acid). Although unsulfated ΔHexUA-GlcNAc is the major disaccharide in both preparations, the proportion of this disaccharide in GPC3-AP is much higher than in GPC5-AP. Conversely, the proportion of sulfated disaccharides is significantly higher in the HS chains purified from GPC5-AP. We have also compared the disaccharide composition of GPC3-AP and GPC5-AP purified from transiently transfected RH30 RMS cells. As in the case of NIH 3T3 cells, we also found a significantly higher proportion of sulfated disaccharides in the HS chains extracted from GPC5-AP (Fig. S2). Consequently, we conclude that GPC5-AP displays a much higher proportion of sulfated disaccharides. Because the binding capacity of a given GAG chain is mostly determined by the degree of sulfation, this result strongly suggests that the higher sulfation of the HS chains of GPC5 is responsible, at least in part, for the larger binding capacity of GPC5 to Ptc1 compared with that of GPC3.

Discussion

In this study, we show that GPC5 stimulates the proliferation of RMS cells by activating Hh signaling. Because GPC5 is overexpressed in RMS (Williamson et al., 2007), this work uncovers

a novel mechanism by which Hh signaling can be activated in this malignancy. In addition, our results strongly suggest that GPC5 promotes this signaling pathway at the cell surface by facilitating/stabilizing the interaction between Hh and Ptc1. Other proteins that stimulate Hh signaling at the cell surface level have already been described, including Cdo, Boc, and Gas1 (Zhang et al., 2006; Allen et al., 2007; Jiang and Hui, 2008; Varjosalo and Taipale, 2008). Although these proteins bind to Hh, the precise mechanism by which they stimulate Hh signaling remains unknown. Given the importance of this signaling pathway in the regulation of differentiation and morphogenesis during development in many tissues, the existence of several membrane proteins that modulate Hh is not surprising.

As discussed in the Introduction, it has been previously shown that Dlp, one of the *Drosophila* glypicans, stimulates Hh signaling (Desbordes and Sanson, 2003; Lum et al., 2003). Although the precise mechanism of this stimulation has not been characterized, it has been proposed that Dlp acts as an Hh coreceptor (Gallet et al., 2008; Yan et al., 2010). It seems therefore that, in the context of Hh signaling, GPC5 behaves functionally like Dlp. However, our results show a clear structural difference between GPC5 and Dlp in the context of Hh signaling: although we found that the GAG chains are essential for GPC5-induced stimulation of Hh signaling, Yan et al. (2010) reported that the GAG chains are not required for Dlp function. This difference could be because the Dlp core protein interacts with Hh (Yan et al., 2010), whereas that of GPC5 does not. In this regard, it is interesting to note that Hh interacts with the core proteins of two glypicans that are cleaved by convertases (GPC3 and Dlp) and that GPC5 is not cleaved by such endoproteases (Eugster et al., 2007).

The idea that proteoglycans can act as coreceptors was first proposed to explain the stimulatory role of these proteins in FGF signaling (Gallagher, 1994). As in the case of GPC5 and Hh, the role of proteoglycans in the context of FGF signaling is mediated by their HS chains, which can interact simultaneously with both the ligand and the receptor (Pellegrini et al., 2000). However, unlike the FGF case, we found that soluble heparin does not mimic the Hh stimulatory activity of the proteoglycan (Fig. S3). This result suggests that the core protein of GPC5 plays an essential role. One possibility is that the GAG chains have to be displayed in a specific relative position in the context of the Hh–Ptc1 complex for a productive interaction and that the core protein of GPC5 plays a critical role in positioning the GAG chains in the context of the ligand receptor complex.

Recent work in *Drosophila* has demonstrated that Hh has to form large oligomeric clusters for long-range signaling and that cell surface HS proteoglycans play a critical role in the formation of these oligomers (Vyas et al., 2008). It could therefore be suggested that GPC5 might also increase Hh signaling by stimulating cluster formation. However, in the signaling experiments described in Figs. 3 and 9, we only tested the effect of GPC5 in the context of autocrine or paracrine signaling. In this context, monomeric Hh has a similar signaling strength than the oligomerized form (Vyas et al., 2008), suggesting that a potential GPC5-induced oligomerization will have no impact on signaling. In fact, we have observed that conditioned medium from GPC5-transfected cells has the same Hh activity in the Gli1 reporter assay than conditioned medium from vector control–transfected cells (unpublished data).

Williams et al. (2010) have recently reported that GPC5 cannot rescue the inhibition of Hh signaling induced by *dlp* RNAi in *Drosophila* cells. These results are apparently contradictory with our findings. It should be noted, however, that *Drosophila* cells do not have cilia. In addition, the authors of this study used an expression vector in which the GPC5 cDNA had a HA tag at the N terminus. We have observed that this tag dramatically inhibits glycanation of GPC5 (unpublished data). In fact, the Western blot analysis of GPC5 included in the study by Williams et al. (2010) shows a poorly glycanated GPC5, with an apparent molecular mass that is not larger than that corresponding to the core protein. As we show here, GPC5 glycanation is essential for its ability to activate Hh signaling.

We have previously reported that GPC3 acts as an inhibitor of Hh activity by competing with Ptc1 for Hh binding (Capurro et al., 2008, 2009). Thus, one important finding of this study is that two members of the glypican family can display opposite roles in the regulation of Hh signaling. We also uncover here the molecular basis for the differential role of GPC3 and GPC5 in the regulation of Hh activity by demonstrating that, unlike GPC3, GPC5 can interact with Ptc1. Interestingly, this interaction is mediated by the GAG chains. This GAG-mediated interaction of GPC5 with Ptc1 was observed not only with GPC5 purified from RMS cells but also with GPC5 purified from nonmalignant NIH 3T3 fibroblasts. Because GPC5 displays CS chains and GPC3 does not, we first hypothesized that the CSs are responsible for the differential interaction. However, binding experiments after digestion with HSase and CSase showed that the interaction between GPC5 and Ptc1 is mostly mediated by the HS chains, although the CS chains can also bind to Ptc1 and contribute to the interaction when the HS chains are present. In this regard, our results are similar to those reported by Deepa et al. (2004), who showed that basic FGF interacts more efficiently with syndecan-4 when this proteoglycan carries CS in addition to HS. Because both GPC5 and GPC3 display HS chains and the sulfation pattern is an important determinant of the binding properties of HS, we then hypothesized that this pattern should be different in these two glypicans. Indeed, as shown in Fig. 9, we found that the HS chains of GPC5 display a significantly higher degree of sulfation than those of GPC3 obtained from the same cell type. Differential sulfation of proteoglycans that are produced by the same cell line has already been reported (Tveit et al., 2005). It is possible that, in certain cell types, there are different kinds of complexes that contain the enzymes involved in GAG synthesis (gagosomes) and that the different proteoglycan core proteins are targeted to specific gagosomes (Victor et al., 2009). It should also be noted that, at this point in time, we cannot discard the possibility that the fact that GPC5 displays more GAG chains than GPC3 also contributes to the differential binding to Ptc1. The length of the HS chains or their fine structure could also be contributing factors.

Another important finding of this study is that GPC5 can localize to cilia. This finding is consistent with our results showing that GPC5 interacts with Ptc1. Currently the molecular

determinants of cilia localization are not clearly understood. However, our finding that very little GPC5ΔGAG mutant can be found in cilia leads us to speculate that the ciliary localization of GPC5 may be the result of its interaction with Ptc1. This possibility is also supported by our observation that GPC3, which does not interact with Ptc1 (Capurro et al., 2008), could not be detected in the cilia (Fig. 7 C). In this regard, it is important to note that the localization of GPC3 outside of the cilium is consistent with the ability of this glypican to compete for Hh with Ptc1 and, in this way, to inhibit Hh signaling. We also speculate that the small amount of GPC5ΔGAG that was detected in the cilia is the result of overexpression in the transfected NIH 3T3 cells. It should be noted, on the other hand, that we could detect high levels of endogenous GPC5 in the cilia of RMS cells (Fig. 7 D).

We show here that the affinity of GPC5 for Shh is significantly lower than that of GPC3. Furthermore, whereas the interaction of GPC3 with Shh is mediated mostly by the core protein (Capurro et al., 2008), GPC5 binds to Shh mainly through the HS chains. Although the lack of high affinity interaction between the core protein of GPC5 and Shh is somewhat unexpected, it should be noted that the Shh-binding domain in GPC3 has not been identified yet and that the two glypicans display only 50% identity. Based on these results, it is reasonable to speculate that the lower affinity of GPC5 for Shh may facilitate a productive interaction of this growth factor with Ptc1, whereas the high affinity interaction between GPC3 and Shh inhibits the engagement of Ptc1 by the ligand.

Because GPC5 is overexpressed in RMS, our finding that this glypican promotes the growth of RMS by stimulating Hh signaling may have clinical implications. Various inhibitors of Hh signaling are currently being tested in clinical trials as tools to treat several cancer types that display increased activation of the Hh signaling pathway (Rudin et al., 2009; Von Hoff et al., 2009). Most of these Hh inhibitors target Smoothened, a key component of the Hh pathway. The results presented here suggest that these inhibitors could also be used to treat RMS patients. Furthermore, if inhibitors of GPC5 activity can be found, a more specific targeting of Hh signaling in RMS could be achieved, avoiding, in this way, potential side effects of a general inhibition of the Hh activity.

Materials and methods

Cell lines and plasmids

293T, NIH 3T3, and C2C12 cells were cultured in DME supplemented with 10% FBS. The RMS cell lines CW9019 and RH30 were grown in RPMI 1640 medium with 10% FBS. All cell lines were maintained at 37°C in a humidified atmosphere with 5% CO_2. To prepare conditioned media, 293T, NIH 3T3, or RH30 cells were transiently transfected with the indicated expression vectors, and culture medium was collected 72 h after transfection. ShhN-conditioned medium was generated by transfecting 293T cells with an Shh expression vector. The medium, which contained 2% serum, was collected 6 d after transfection. The multimeric ShhN peptide–conditioned medium was generated by transfecting the full-length Shh cDNA into 293T cells. The medium was collected after 48 h in serum-free conditions.

The full-length human GPC5 DNA was obtained from OriGene Technologies and cloned into pTracer (Invitrogen). A nonglycanated mutant of GPC5 (GPC5ΔGAG) was generated by mutating five serine residues (Ser^{441}, Ser^{486}, Ser^{495}, Ser^{507}, and Ser^{509}) to alanine by site-directed mutagenesis. Mutations were verified by DNA sequencing. The GPC5-AP and GPC5ΔGAG-AP vectors were prepared by inserting the human GPC5 and GPC5ΔGAG cDNAs into the BspE1 site of the pAP-Tag2 vector (GeneHunter Corporation). The other expression vectors used in this study (Shh, ShhN, GPC3, and HA-tagged Ptc1) were previously described (Capurro et al., 2008).

Generation of the GPC5-overexpressing RMS cell line CW9019

CW9019 cells were transfected with an expression vector containing the full-length wild-type GPC5 cDNA and a selectable marker or with the selectable vector alone (pTracer). The transfections were performed by using Lipofectamine 2000 (Invitrogen) according to the manufacturer's instructions. After selection, cells were expanded and stained with the anti-GPC5 mAb MAB2607 (R&D Systems) and an FITC-conjugated secondary antibody. GPC5-overexpressing cells were then isolated by FACS.

siRNA treatment

RH30 cells were plated at 2×10^5 cells per well on 6-well tissue culture dishes in RPMI 1640 containing 10% FBS without antibiotics. The next day, the cells were transfected with 100-nM SMARTpool siRNAs for GPC5 or nontargeting siRNA (Thermo Fisher Scientific) by using Lipofectamine 2000.

Cell proliferation assay

Cells were plated at 3,000 cells per well on 96-well tissue culture plates in RPMI 1640 containing 1% FBS, and cell numbers were assessed at the indicated time points (Figs. 1 C and 2 C) using the MTT assay. In brief, 5 µl MTT stock solution containing 5 mg/ml 3-(4,5-dimethylthiazol-2-yl)-2,5-diphenyltetrazolium bromide in water was added to each well and incubated at 37°C for 4 h. After removing the medium, 100 µl DMSO was added into each well to dissolve the formazan by pipetting up and down several times, and then the absorbance was measured at 570 nm. Each experiment was performed at least three times by quintuplicates.

Real-time RT-PCR

Total mRNA was extracted from cells using the TRIZOL reagent (Invitrogen) according to the manufacturer's instructions. The mRNA was then used as a template to prepare cDNA using Superscript II Reverse Transcriptase and oligo(dT)12–18 primers (Invitrogen). Quantification of Gli1 mRNA expression was performed on a real-time PCR instrument (LightCycler 3.5; Roche) using SYBR green (QuantiTect; QIAGEN). Sequences of the oligonucleotide primers used for human Gli1 and β-actin are as follows: Gli1 forward, 5′-AGGGAGGAAAGCAGACTGAC-3′, and reverse, 5′-CCAGTCATTTCCACACCACT-3′; and β-actin forward, 5′-TTCTACAATGAGCTGCGTGTG-3′, and reverse, 5′-GGGGTGTTGAAGGTCTCAAA-3′. Values for each sample were normalized by the level of β-actin in a parallel RNA sample. Each RNA preparation was analyzed in triplicate. To express values as a percentage, the control value was set at 100%. All error bars represent SDs based on the means of three independent trials. Probability of a significant difference between two values was determined by a paired two-tailed Student's *t* test. Values were considered to be statistically significant when $P < 0.05$.

Purification of glypicans

Cell surface–anchored GPC5 was purified by anion-exchange chromatography on DEAE-Sepharose (GE Healthcare) as previously described (Herndon and Lander, 1990) except that the concentration of NaCl in the elution buffer was increased to 2 M. Secreted AP-tagged glypicans were purified from conditioned media by two successive steps: first, anion-exchange chromatography on DEAE-Sepharose and, second, affinity chromatography with the anti-AP mAb coupled to agarose (Sigma-Aldrich). In brief, the DEAE-Sepharose gel was added to the conditioned medium and incubated at 4°C for 4 h. The suspension was then collected in an empty column and washed with 0.2-M NaCl in 50-mM phosphate buffer, pH 6.5, and the bound material was eluted with 2-M NaCl in 50-mM phosphate buffer, pH 6.5. The eluate was diluted fourfold with H_2O and loaded on a column containing anti-AP agarose. After washing the column with 0.5-M NaCl in 50-mM Tris buffer (first wash at pH 8.0 and second wash at pH 9.0), the AP-tagged glypican was eluted with 100-mM triethylamine and was immediately neutralized by 1-M NaH_2PO_4. Finally, all glypican preparations were desalted by using Microcon YM-10 (Millipore).

Hh reporter assay

Cells were seeded into 6-well plates and cotransfected with a reporter plasmid in which luciferase expression is driven by a promoter containing Gli1-binding sequences (Capurro et al., 2008) and other indicated plasmids. 1 d after transfection, cells were transferred to 24-well plates, and the following day, ShhN- or control-conditioned medium (diluted 1:10 in

DME–2% FBS) was added for 48 h. Cells were then lysed, and luciferase activity was measured.

Immunoprecipitations and Western blots

Transfected 293T cells were lysed using radioimmunoprecipitation assay buffer containing protease inhibitors, and the cell lysates were precleared with protein G–Sepharose. Immunoprecipitations were performed overnight, and the immunoprecipitates were analyzed by Western blotting. Antibodies used in this study were mouse anti-GPC5 mAb MAB2607 (R&D Systems), mouse anti-HA mAb 12CA5 (Roche), and rabbit anti-Ptc1 polyclonal antibody H-267 (Santa Cruz Biotechnology, Inc.).

Binding assay

293T cells were transfected with a HA-tagged Ptc1 vector. 2 d after transfection, cells were lysed, and Ptc1 was immunoprecipitated from the lysate with an anti-HA antibody (12CA5) bound to protein G–Sepharose beads. The beads were then blocked with 5% BSA in PBS containing 0.1% Triton X-100 for 1 h and incubated with various AP-tagged ligands or AP alone for 1 h at room temperature. After the beads were washed three times with 20-mM Hepes buffer, pH 7.4, containing 0.15-M NaCl and 0.5% Tween 20, the AP activities of the various ligands bound to the beads were measured with a p-Nitrophenyl phosphate tablet set (SIGMAFAST; Sigma-Aldrich). The background binding was measured by incubating the beads with lysates of 293T cells transfected with an AP vector control, and it was subtracted from each sample measurement. To measure the affinity of the GPC5–Ptc1 interaction, the Ptc1-bound beads were incubated with 200 µl of conditioned media containing various concentrations of GPC5-AP at 25°C for 1 h, and the bound AP activity was measured as described in this section. The K_d value was obtained from a Scatchard analysis of the binding data.

SPR analysis

The kinetic constants of the interaction of Shh with GPC5 were measured using a biosensor system (Biacore 3000; GE Healthcare). 15 µg of soluble GPC5-AP fusion protein, which was purified from the conditioned medium of GPC5-AP–transfected 293T cells, was biotinylated with EZ-Link Sulfo-NHS-LC-Biotin reagent (Thermo Fisher Scientific), and one third of the biotinylated GPC5-AP was treated with HSase II and CSase ABC in the presence of protease inhibitors to remove GAG chains. Glycanated and nonglycanated GPC5-AP were individually immobilized (1,000 response units) in flow cells 2 and 3 on a sensorchip (SA; GE Healthcare). A similar amount of biotinylated AP was immobilized in flow cell 1 to use as a correction reference for nonspecific binding. The indicated concentrations of ShhN (R&D Systems) in running buffer HBS-EP (10-mM Hepes, pH 7.4, 150-mM NaCl, 3-mM EDTA, and 0.005% surfactant P20; GE Healthcare) were injected over flow cells at 30 ml/min for 90 s at 25°C. After a 3-min wash with HBS-EP, the flow cells were regenerated with 1-min pulses of HBS-EP containing 2-M NaCl.

Analysis of the GAG chains

Purified glypicans were treated with CSase ABC (Sigma-Aldrich) or HSase (IBEX Technologies, Inc.). For binding assays and Western blot analysis, an aliquot of purified glypican was treated with 0.5 mIU CSase ABC or HSase II in 20 µl of 20-mM acetate-NaOH buffer, pH 7.0, containing 10-mM $Ca(OAc)_2$ and protease inhibitors at 37°C for 1 h. Enzymatic treatments for analysis of the disaccharide composition of GAG chains were performed as previously described (Deepa et al., 2004). In brief, an aliquot (1 µg of protein) of purified GPC3-AP or GPC5-AP from transiently transfected NIH 3T3 or RH30 cells was subjected to digestion with a mixture of HSase I and III. The digest was labeled with 2AB and subjected to anion-exchange HPLC on an amine-bound silica PA-03 column (Pack PA; YMC Co., Ltd.).

Confocal microscopy

NIH 3T3 cells were plated on poly-L-lysine–coated coverslips and transfected with the indicated expression vectors. 2 d after transfection, the confluent cells were starved in FBS-free DME for 2 h, washed three times with ice-cold PBS, fixed in 4% paraformaldehyde/PBS, and permeabilized with 0.1% Triton X-100 for 15 min at room temperature. GPC5, GPC3, and cilia were detected with biotinylated mouse anti-GPC5 mAb (MAB2607; R&D Systems), Alexa Flour 546–conjugated mouse anti-GPC3 (1G12), and mouse antiacetylated tubulin mAb (T7451; Sigma-Aldrich), respectively. Immunostaining was performed as previously described (Capurro et al., 2008). To detect the cilia in RMS cells, RH30 cells were plated on poly-L-lysine–coated coverslips and were starved in FBS-free RPMI 1640 for 48 h before fixing for staining. Stained cells were photographed on a microscope (Axiovert 100M; Carl Zeiss, Inc.) equipped with a Plan Apochromat (Carl Zeiss, Inc.) 100×/1.4 NA oil dichromic objective. Confocal images were generated using a scanning laser microscope (LSM 510 version 3.2 SP2; Carl Zeiss, Inc.). Image analysis was performed using the ImageJ program (National Institutes of Health) as previously reported (Rohatgi et al., 2007). In brief, a mask, which was constructed by manually outlining cilia in the image of acetylated tubulin staining, was applied to GPC5/GPC5ΔGAG-stained images to measure the fluorescence intensity at cilia. The mean fluorescence intensity of other regions of the cell was obtained by measuring several representative regions on the cell by moving the mask. After subtracting the background from both aforementioned fluorescence intensities, the ratio of fluorescence intensity in the cilium to that outside of the cilium was calculated.

Online supplemental material

Fig. S1 shows a luciferase reporter assay in NIH 3T3 cells demonstrating that GPC5 stimulates both ShhN and full-length Shh signaling. Fig. S2 shows the disaccharide analysis of the HS chains of GPC3-AP and GPC5-AP purified from transiently transfected RH30 cells. Fig. S3 demonstrates that heparan does not stimulate Shh-induced signaling as measured by a luciferase reporter assay in NIH 3T3 cells. Table S1 shows the kinetic parameters for the interaction of Shh with GPC5-AP. Online supplemental material is available at http://www.jcb.org/cgi/content/full/jcb.201008087/DC1.

This work was funded by the Canadian Institute of Health Research.

Submitted: 13 August 2010
Accepted: 24 January 2011

References

Akiyama, T., K. Kamimura, C. Firkus, S. Takeo, O. Shimmi, and H. Nakato. 2008. Dally regulates Dpp morphogen gradient formation by stabilizing Dpp on the cell surface. *Dev. Biol.* 313:408–419. doi:10.1016/j.ydbio.2007.10.035

Allen, B.L., T. Tenzen, and A.P. McMahon. 2007. The Hedgehog-binding proteins Gas1 and Cdo cooperate to positively regulate Shh signaling during mouse development. *Genes Dev.* 21:1244–1257. doi:10.1101/gad.1543607

Beckett, K., X. Franch-Marro, and J.P. Vincent. 2008. Glypican-mediated endocytosis of Hedgehog has opposite effects in flies and mice. *Trends Cell Biol.* 18:360–363. doi:10.1016/j.tcb.2008.06.001

Bishop, J.R., M. Schuksz, and J.D. Esko. 2007. Heparan sulphate proteoglycans fine-tune mammalian physiology. *Nature*. 446:1030–1037. doi:10.1038/nature05817

Breitfeld, P.P., and W.H. Meyer. 2005. Rhabdomyosarcoma: new windows of opportunity. *Oncologist*. 10:518–527. doi:10.1634/theoncologist.10-7-518

Bridge, J.A., J. Liu, V. Weibolt, K.S. Baker, D. Perry, R. Kruger, S. Qualman, F. Barr, P. Sorensen, T. Triche, and R. Suijkerbuijk. 2000. Novel genomic imbalances in embryonal rhabdomyosarcoma revealed by comparative genomic hybridization and fluorescence in situ hybridization: an intergroup rhabdomyosarcoma study. *Genes Chromosomes Cancer*. 27:337–344. doi:10.1002/(SICI)1098-2264(200004)27:4<337::AID-GCC1>3.0.CO;2-1

Capurro, M.I., P. Xu, W. Shi, F. Li, A. Jia, and J. Filmus. 2008. Glypican-3 inhibits Hedgehog signaling during development by competing with patched for Hedgehog binding. *Dev. Cell*. 14:700–711. doi:10.1016/j.devcel.2008.03.006

Capurro, M.I., F. Li, and J. Filmus. 2009. Overgrowth of a mouse model of Simpson-Golabi-Behmel syndrome is partly mediated by Indian hedgehog. *EMBO Rep.* 10:901–907. doi:10.1038/embor.2009.98

Deepa, S.S., S. Yamada, M. Zako, O. Goldberger, and K. Sugahara. 2004. Chondroitin sulfate chains on syndecan-1 and syndecan-4 from normal murine mammary gland epithelial cells are structurally and functionally distinct and cooperate with heparan sulfate chains to bind growth factors. A novel function to control binding of midkine, pleiotrophin, and basic fibroblast growth factor. *J. Biol. Chem.* 279:37368–37376. doi:10.1074/jbc.M403031200

Desbordes, S.C., and B. Sanson. 2003. The glypican Dally-like is required for Hedgehog signalling in the embryonic epidermis of *Drosophila*. *Development*. 130:6245–6255. doi:10.1242/dev.00874

Eugster, C., D. Panáková, A. Mahmoud, and S. Eaton. 2007. Lipoprotein-heparan sulfate interactions in the Hh pathway. *Dev. Cell*. 13:57–71. doi:10.1016/j.devcel.2007.04.019

Filmus, J., and S.B. Selleck. 2001. Glypicans: proteoglycans with a surprise. *J. Clin. Invest.* 108:497–501.

Filmus, J., W. Shi, Z.M. Wong, and M.J. Wong. 1995. Identification of a new membrane-bound heparan sulphate proteoglycan. *Biochem. J.* 311:561–565.

Filmus, J., M. Capurro, and J. Rast. 2008. Glypicans. *Genome Biol.* 9:224. doi:10.1186/gb-2008-9-5-224

Gallagher, J.T. 1994. Heparan sulphates as membrane receptors for the fibroblast growth factors. *Eur. J. Clin. Chem. Clin. Biochem.* 32:239–247.

Gallet, A., L. Staccini-Lavenant, and P.P. Thérond. 2008. Cellular trafficking of the glypican Dally-like is required for full-strength Hedgehog signaling and wingless transcytosis. *Dev. Cell*. 14:712–725. doi:10.1016/j.devcel.2008.03.001

Gorlin, R.J. 2004. Nevoid basal cell carcinoma (Gorlin) syndrome. *Genet. Med.* 6:530–539. doi:10.1097/01.GIM.0000144188.15902.C4

Gorsi, B., and S.E. Stringer. 2007. Tinkering with heparan sulfate sulfation to steer development. *Trends Cell Biol.* 17:173–177. doi:10.1016/j.tcb.2007.02.006

Hahn, H., C. Wicking, P.G. Zaphiropoulous, M.R. Gailani, S. Shanley, A. Chidambaram, I. Vorechovsky, E. Holmberg, A.B. Unden, S. Gillies, et al. 1996. Mutations of the human homolog of *Drosophila* patched in the nevoid basal cell carcinoma syndrome. *Cell*. 85:841–851. doi:10.1016/S0092-8674(00)81268-4

Hahn, H., L. Wojnowski, A.M. Zimmer, J. Hall, G. Miller, and A. Zimmer. 1998. Rhabdomyosarcomas and radiation hypersensitivity in a mouse model of Gorlin syndrome. *Nat. Med.* 4:619–622. doi:10.1038/nm0598-619

Han, C., T.Y. Belenkaya, B. Wang, and X. Lin. 2004. *Drosophila* glypicans control the cell-to-cell movement of Hedgehog by a dynamin-independent process. *Development*. 131:601–611. doi:10.1242/dev.00958

Herndon, M.E., and A.D. Lander. 1990. A diverse set of developmentally regulated proteoglycans is expressed in the rat central nervous system. *Neuron*. 4:949–961. doi:10.1016/0896-6273(90)90148-9

Jackson, S.M., H. Nakato, M. Sugiura, A. Jannuzi, R. Oakes, V. Kaluza, C. Golden, and S.B. Selleck. 1997. dally, a *Drosophila* glypican, controls cellular responses to the TGF-beta-related morphogen, Dpp. *Development*. 124:4113–4120.

Jiang, J., and C.C. Hui. 2008. Hedgehog signaling in development and cancer. *Dev. Cell*. 15:801–812. doi:10.1016/j.devcel.2008.11.010

Kiprilov, E.N., A. Awan, R. Desprat, M. Velho, C.A. Clement, A.G. Byskov, C.Y. Andersen, P. Satir, E.E. Bouhassira, S.T. Christensen, and R.E. Hirsch. 2008. Human embryonic stem cells in culture possess primary cilia with hedgehog signaling machinery. *J. Cell Biol.* 180:897–904. doi:10.1083/jcb.200706028

Kreuger, J., L. Perez, A.J. Giraldez, and S.M. Cohen. 2004. Opposing activities of Dally-like glypican at high and low levels of Wingless morphogen activity. *Dev. Cell*. 7:503–512. doi:10.1016/j.devcel.2004.08.005

Lin, X., and N. Perrimon. 1999. Dally cooperates with *Drosophila* Frizzled 2 to transduce Wingless signalling. *Nature*. 400:281–284. doi:10.1038/22343

Lum, L., S. Yao, B. Mozer, A. Rovescalli, D. Von Kessler, M. Nirenberg, and P.A. Beachy. 2003. Identification of Hedgehog pathway components by RNAi in *Drosophila* cultured cells. *Science*. 299:2039–2045. doi:10.1126/science.1081403

Milenkovic, L., M.P. Scott, and R. Rohatgi. 2009. Lateral transport of Smoothened from the plasma membrane to the membrane of the cilium. *J. Cell Biol.* 187:365–374. doi:10.1083/jcb.200907126

Ohkawara, B., T.S. Yamamoto, M. Tada, and N. Ueno. 2003. Role of glypican 4 in the regulation of convergent extension movements during gastrulation in *Xenopus laevis*. *Development*. 130:2129–2138. doi:10.1242/dev.00435

Paine-Saunders, S., B.L. Viviano, and S. Saunders. 1999. GPC6, a novel member of the glypican gene family, encodes a product structurally related to GPC4 and is colocalized with GPC5 on human chromosome 13. *Genomics*. 57:455–458. doi:10.1006/geno.1999.5793

Pellegrini, L., D.F. Burke, F. von Delft, B. Mulloy, and T.L. Blundell. 2000. Crystal structure of fibroblast growth factor receptor ectodomain bound to ligand and heparin. *Nature*. 407:1029–1034. doi:10.1038/35039551

Rohatgi, R., L. Milenkovic, and M.P. Scott. 2007. Patched1 regulates hedgehog signaling at the primary cilium. *Science*. 317:372–376. doi:10.1126/science.1139740

Rudin, C.M., C.L. Hann, J. Laterra, R.L. Yauch, C.A. Callahan, L. Fu, T. Holcomb, J. Stinson, S.E. Gould, B. Coleman, et al. 2009. Treatment of medulloblastoma with hedgehog pathway inhibitor GDC-0449. *N. Engl. J. Med.* 361:1173–1178. doi:10.1056/NEJMoa0902903

Ruiz i Altaba, A., C. Mas, and B. Stecca. 2007. The Gli code: an information nexus regulating cell fate, stemness and cancer. *Trends Cell Biol.* 17:438–447. doi:10.1016/j.tcb.2007.06.007

Saunders, S., S. Paine-Saunders, and A.D. Lander. 1997. Expression of the cell surface proteoglycan glypican-5 is developmentally regulated in kidney, limb, and brain. *Dev. Biol.* 190:78–93. doi:10.1006/dbio.1997.8690

Song, H.H., and J. Filmus. 2002. The role of glypicans in mammalian development. *Biochim. Biophys. Acta*. 1573:241–246.

Song, H.H., W. Shi, Y.Y. Xiang, and J. Filmus. 2005. The loss of glypican-3 induces alterations in Wnt signaling. *J. Biol. Chem.* 280:2116–2125. doi:10.1074/jbc.M410090200

Sugahara, K., T. Mikami, T. Uyama, S. Mizuguchi, K. Nomura, and H. Kitagawa. 2003. Recent advances in the structural biology of chondroitin sulfate and dermatan sulfate. *Curr. Opin. Struct. Biol.* 13:612–620. doi:10.1016/j.sbi.2003.09.011

Tostar, U., C.J. Malm, J.M. Meis-Kindblom, L.G. Kindblom, R. Toftgård, and A.B. Undén. 2006. Deregulation of the hedgehog signalling pathway: a possible role for the PTCH and SUFU genes in human rhabdomyoma and rhabdomyosarcoma development. *J. Pathol.* 208:17–25. doi:10.1002/path.1882

Tsuda, M., K. Kamimura, H. Nakato, M. Archer, W. Staatz, B. Fox, M. Humphrey, S. Olson, T. Futch, V. Kaluza, et al. 1999. The cell-surface proteoglycan Dally regulates Wingless signalling in *Drosophila*. *Nature*. 400:276–280. doi:10.1038/22336

Tveit, H., G. Dick, V. Skibeli, and K. Prydz. 2005. A proteoglycan undergoes different modifications en route to the apical and basolateral surfaces of Madin-Darby canine kidney cells. *J. Biol. Chem.* 280:29596–29603. doi:10.1074/jbc.M503691200

Varjosalo, M., and J. Taipale. 2008. Hedgehog: functions and mechanisms. *Genes Dev.* 22:2454–2472. doi:10.1101/gad.1693608

Veugelers, M., B. De Cat, H. Ceulemans, A.M. Bruystens, C. Coomans, J. Dürr, J. Vermeesch, P. Marynen, and G. David. 1999. Glypican-6, a new member of the glypican family of cell surface heparan sulfate proteoglycans. *J. Biol. Chem.* 274:26968–26977. doi:10.1074/jbc.274.38.26968

Victor, X.V., T.K.N. Nguyen, M. Ethirajan, V.M. Tran, K.V. Nguyen, and B. Kuberan. 2009. Investigating the elusive mechanism of glycosaminoglycan biosynthesis. *J. Biol. Chem.* 284:25842–25853. doi:10.1074/jbc.M109.043208

Von Hoff, D.D., P.M. LoRusso, C.M. Rudin, J.C. Reddy, R.L. Yauch, R. Tibes, G.J. Weiss, M.J. Borad, C.L. Hann, J.R. Brahmer, et al. 2009. Inhibition of the hedgehog pathway in advanced basal-cell carcinoma. *N. Engl. J. Med.* 361:1164–1172. doi:10.1056/NEJMoa0905360

Vyas, N., D. Goswami, A. Manonmani, P. Sharma, H.A. Ranganath, K. VijayRaghavan, L.S. Shashidhara, R. Sowdhamini, and S. Mayor. 2008. Nanoscale organization of hedgehog is essential for long-range signaling. *Cell*. 133:1214–1227. doi:10.1016/j.cell.2008.05.026

Williams, E.H., W.N. Pappano, A.M. Saunders, M.S. Kim, D.J. Leahy, and P.A. Beachy. 2010. Dally-like core protein and its mammalian homologues mediate stimulatory and inhibitory effects on Hedgehog signal response. *Proc. Natl. Acad. Sci. USA*. 107:5869–5874. doi:10.1073/pnas.1001777107

Williamson, D., J. Selfe, T. Gordon, Y.J. Lu, K. Pritchard-Jones, K. Murai, P. Jones, P. Workman, and J. Shipley. 2007. Role for amplification and expression of glypican-5 in rhabdomyosarcoma. *Cancer Res.* 67:57–65. doi:10.1158/0008-5472.CAN-06-1650

Yan, D., Y. Wu, Y. Yang, T.Y. Belenkaya, X. Tang, and X. Lin. 2010. The cell-surface proteins Dally-like and Ihog differentially regulate Hedgehog signaling strength and range during development. *Development*. 137:2033–2044. doi:10.1242/dev.045740

Zhang, W., J.S. Kang, F. Cole, M.J. Yi, and R.S. Krauss. 2006. Cdo functions at multiple points in the Sonic Hedgehog pathway, and Cdo-deficient mice accurately model human holoprosencephaly. *Dev. Cell*. 10:657–665. doi:10.1016/j.devcel.2006.04.005